

Similarity-Based Neural Network Model for FBIR System of Optical Satellite Image Quality Assessment

Saurabh Srivastava^a, Tasneem Ahmed^b

^{a,b} Advanced Computing and Research Laboratory, Department of Computer Application, Integral University, Lucknow, Uttar Pradesh, India

Article History: Received: 11 January 2021; Revised: 12 February 2021; Accepted: 27 March 2021; Published online: 4 June 2021

Abstract: Satellite images are an important tool of Earth observation, as well as for observing man-made and natural resources. Multiple satellites are in space, providing numerous images on a daily/weekly basis for land surface interpretation, study, and various type of monitoring. Satellite images are a significant source of evidence and information used in a variety of areas, including environmental impact measurement, agricultural tracking, woodland survey, and identification of changes in urban areas. It is still a difficult task to retrieve a noise-free image from an image repository and extract meaningful information from an image, especially optical satellite images that may be weather effected, which are less capable to generate efficient and accurate results for earth surface monitoring particularly when the image contains multiple semantic information. Many researchers have developed different neural network models for similarity measurement that are capable of finding similarity between two patterns in the literature, but finding similarity between two satellite images is a difficult challenge since satellite images relate to normal datasets. In this paper, a similarity-based neural network (SBNN) model for the FBIR system has been developed. The SBNN model is a replacement for the KNN algorithm, which was proposed in our previous study. The SBNN model calculates the image band similarity between the required image and the referenced image, and based on band similarity, the system predicts that the image is suitable for post-processing or not. The improved version of the FBIR system (i.e. FBIR with SBNN model) allows the retrieval of pre-processed band data of the image as per user requirement. The proposed FBIR system minimizes the downloading time, wastage of the internet, and the most important thing is the time of the user that is consumed during the pre-processing of raw images. The main advantage of SBNN based FBIR system is that there will not be a need to download a complete image (i.e. composite image of all the respective bands), user can select the required individual band image and can easily download it through a user-friendly GUI. In future, SBNN based FBIR model can be very beneficent for the scientist and environmentalist to conduct quick case studies for urban heat mapping, precision agriculture, coal fire monitoring and forest fire mapping, etc..

Keywords: FBIR, SBNN, Feature Extraction, Feature Matching, Optical Images, Image Retrieval

1. Introduction

A satellite image contains multi-band data, and each band of the image holds some specific information about the earth's surface so the image takes a large volume in memory to store. Many image retrieval systems are providing satellite images for earth surface monitoring. For retrieval, the user simply requests and the system allows retrieving the image. The traditional image retrieval systems are less capable to indicate the image quality before the retrieval, and always allow to retrieve complete raw image so the retrieval of an image takes time. Most of the time, no need for a complete image (all bands) but during retrieval user has no option to customize the retrieval. After the retrieval of an image, the user can decide that image is suitable for post-processing or not and prepare the image for post-processing. In this study, developed a similarity-based neural network model for the FBIR system which is capable to find the similarity between two satellite images using satellite image features. The SBNN model calculates the similarity between referenced image and the required image, and the FBIR system predicts that the image is suitable for post-processing or not using the similarity result of the SBNN model.

Artificial neural networks (ANN) are the computing model that is inspired by biological neural networks and provide new directions to solve problems arising in a natural task (Sharma et al., 2013). The ANN compose simple processing nodes and connections between them (Ahmed et al., 2015). The connection between two nodes has some weight that is used to determine how much one node will affect the other (Wong et al., 2006). The ANN is usually implemented using electronic components and/or simulated on a digital computer. It employs massive interconnection of simple computing cells called "Neurons" or "Processing Element". It resembles the brain in two ways which are given below (Sharma et al., 2013).

1. Knowledge is acquired by the network through the learning process (Sharma et al., 2013).
2. Interneuron connection strengths (synaptic weights) are responsible for storing knowledge. The way of synaptic weights change defines the architecture of ANNs (Sharma et al., 2013).

The image is a 2D projection of the visual 3D world so some information is lost during the mapping of the image. The features of an image play an important role in technological advancements, especially in the field of image retrieval system (Bunte et al., 2011). The feature-based image retrieval (FBIR) systems are similarity-based

systems, where measure the similarity between two images using similarity measurement algorithms (ElAlami et al., 2014). Feature-based technology is focusing on image retrieval in recent years. Early, feature-based technology mainly leveraged low-level features of the image such as colour, texture, and shape. Traditional similarity measurement techniques are not suitable for large-scale images (Wang et al., 2019). The two basic responsibilities of the FBIR system are indexing and searching. In indexing, extracts the features of the images and store them in a feature vector (Malik et al., 2013). In searching, referenced image feature vector compared with all feature vectors that are extracted from of feature database using similarity measurement algorithm for retrieval of most similar images of the referenced image from the image repository (Malik et al., 2013).

The Color features can be effortlessly obtained from pixel intensities. It is used to describe colour histograms over the whole image, and calculated by the average and standard deviation of the colour intensity of each colour component (Sutojo et al., 2017). Colour features include the colour histogram, colour correlogram, dominant colour descriptor, the colour coherence vector, the colour co-occurrence matrix, vector quantization, and colour moment (ElAlami et al., 2014). The texture features are derived from the grey-level co-occurrence matrix, the Tamura feature, wavelet coefficients, and Gabor filter (Huang et al., 2010). The texture feature is a low-level feature of an image. It is used to describe the detail of the spatial distribution of different patterns in an image such as the spatial arrangement of colour and intensities in an image (Kaur et al., 2017). The shape features are normalized inertia, Zernike moments, the histogram of edge direction, an edge map (ElAlami et al., 2014). Shape features are less developed to compare than colour and texture features of an image because of the inherent complexity of representing shapes (Kaur et al., 2017). It is used to describe the shape of the different regions present in an image such as external boundary, outline, and external surface (Kaur et al., 2017). In comparison among them, colour features are very stable and robust. It is not sensitive to rotation, translation, and scale changes. Moreover, the colour feature calculation is relatively simple (ElAlami et al., 2014).

Many researchers have been used different neural network architectures to build an optimal neural network model for better prediction (Wong et al., 2006). An artificial neural network is a well-known powerful tool in the area of similarity measurement, various types of neural network techniques have been developed for image processing because of their generation ability (ElAlami et al., 2014). Lots of similarity measurement techniques used in image retrieval systems such as Euclidean distance, weighted Euclidean distance, Manhattan distance, cross-correlation distance, minimum mean distance rule, and statistical distance are the most common metrics used to measure the distance between two points in multi-dimensional space (ElAlami et al., 2014). Many similarity measurement algorithms are available that can produce an efficient result, but find the similarity between two satellite images is a complicated task. Satellite images are the major source of data and information that is used in various fields such as environmental impact analysis, forest survey, and ruler to urban change detection (Sharma et al., 2013). Satellite images are the widely available source for mapping and monitoring land use and land cover. Due to rapid development in an urban area (urbanization), land cover around many world's urban areas is quickly changing than ever before (Rasul et al., 2018). Extract information between two images is a very challenging task (Sharma et al., 2013). Especially, when the image shares multiple semantic information.

The improved version of FBIR (FBIR with SBNN) gives the authority to the user that they can select the required band data during retrieval, and the system serves the pre-processed data as per user selection. The new FBIR system minimizes the downloading time, wastage of the internet, and the most important thing is the time of the user that is consumed during the pre-processing of raw images.

2. Study Area and Satellite Data Used

2.1. Study Area

Lucknow city has been considered as a study area in this study, Lucknow is the capital of Uttar Pradesh, India and another popular name of this city is "NAWAVO KA SHAHAR". The study area is located between latitude 26.945746° to 26.734630° and longitude between 80.74451° to 81.142585° and it covers Lucknow city and its nearby areas, the Google Earth image of the study area is shown in Figure 1.

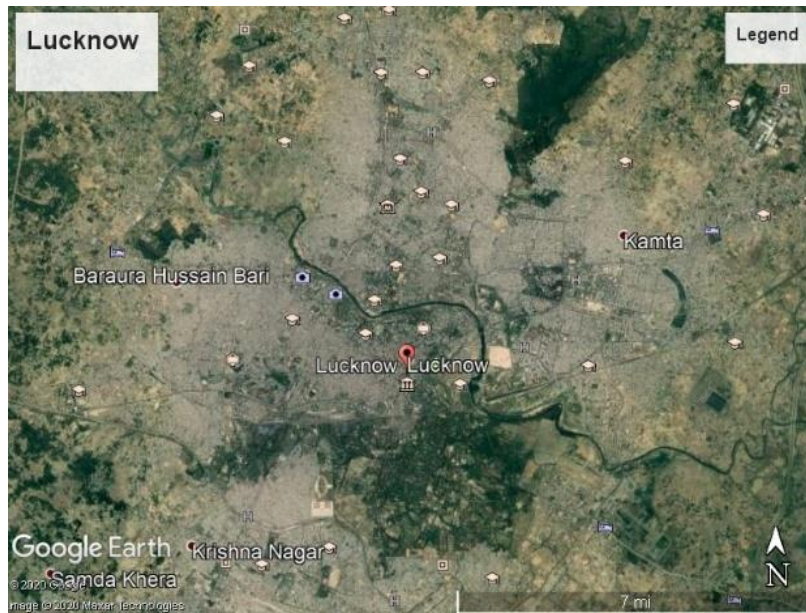


Figure.1 Google Earth Image of Lucknow City.

2.2. Satellite Data Used

In this study, Landsat-8 OLI and Sentinel-2 images are taken to develop and test the SBNN based FBIR system. The details of both the images follow as:

2.2.1.Landsat 8

The most commonly used optical satellite images are Landsat images which have been used for various applications such as agriculture monitoring, geology, forestry, regional planning, land cover, and land classification, etc. The first satellite of the Landsat series launched in 1972 (Demirkesena et al., 2004). Landsat-8 images are undertaken which is the latest and eighth satellite of the Landsat series launched on February 11, 2013, and the seventh satellite that successfully reached orbit. Landsat-8 is the product of the USGS EROS Centre, and it holds an operational land imager (OLI) and thermal infrared sensor (TIRS) with 11 multi-spectral bands. The Ultra blue (Coastal/Aerosol), Blue, Green, Red, Near-Infrared (NIR), 2-Shortwave Infrared (SWIR), Cirrus bands are with 30-meter spatial resolution, Panchromatic band is with 15 meters, while 2-Thermal Infrared (TIRS) bands are available with 100-meter spatial resolution and the revisit time (temporal resolution) of Landsat -8 is 16 days (Yuan et al., 2019).

2.2.2.Sentinel2

Sentinel is a European radar imaging satellite launched by European Space Agency (ESA) which is providing images in all light and weather conditions. Sentinel aims to replace the current order of earth observation mission which is ready to retire in the future. Sentinel-2 was launched on June 23, 2015, and operated by ESA. It carries 13 spectral bands including S-Band (TT & C Support), X-Band, and optical layer through EDRS (data acquisition) with 10-meters, 20-meters, and 60-meter spatial resolution, and its revisit time is 10 days (5 days from 2 satellite) (Sutojo et al., 2017). The potential use of Sentinel images in the land monitoring of forests, water soil and agriculture Emergency mapping, natural disasters marine monitoring, Sea vessel detection and climate change monitoring (Kaur et al., 2017).

In this study, approximately 140 Landsat 8 OLI raw satellite images have been downloaded. Some of the details of Landsat images such as acquisition ID and acquisition dates are shown in table 1.

Sr No.	Sensor	Acquisition ID	Acquisition Date	Image ID
1	Sentinel-2	L1C_T44RMQ_A012057_20190628T052051	06/28/2019	Img_1
2	Sentinel-2	L1C_T44RMQ_A011199_20190429T051605	04/29/2019	Img_2
3	Landsat-8	LC08_L1TP_144041_20180121_20180206_01_T1	1/21/2018	Img_3
4	Landsat-8	LC08_L1TP_144041_20181223_20181227_01_T1	12/23/2018	Img_4
5	Landsat-8	LC08_L1TP_144041_20190209_20190221_01_T1	2/9/2019	Img_5

		T1		
6	Landsat-8	LC08_L1TP_144041_20190617_20190620_01_T1	6/17/2019	Img_6
7	Landsat-8	LC08_L1TP_144041_20190313_20190313_01_RT	3/13/2019	Img_7
8	Landsat-8	LC08_L1TP_144041_20190329_20190404_01_T1	3/29/2019	Img_8
9	Landsat-8	LC08_L1TP_144041_20191210_20191217_01_T1	12/10/2019	Img_9
10	Landsat-8	LC08_L1TP_144041_20200127_20200210_01_T1	1/27/2020	Img_10
11	Landsat-8	LC08_L1TP_144041_20200212_20200225_01_T1	2/12/2020	Img_11
12	Landsat-8	LC08_L1TP_144041_20200416_20200416_01_RT	4/16/2020	Img_12

Table.1. Satellite images used for FBIR development.

3. Theoretical Background

3.1. Pre-processing of Satellite Image

Pre-processing of Landsat-8 image includes the radiometric calibration of the image and creation of true-colour composite image and in Sentinel-2, no need for the radiometric calibration. The radiometric calibration process involves converting the raw signal from a detector into the expected at-aperture spectral radiance/reflectance. The raw signal is expressed as 12-bit digital numbers as a result of the focal plane electronics (Montanaro et al., 2014). A large part of the success of the satellite program can be attributed to the knowledge of the radiometric properties of the satellite sensors. The radiometric calibration helps to characterize the operation of the satellite sensors, but, also allows the full satellite data set to be used in a quantitative sense for such applications as land use and land-cover change (Thome et al., 2011).

True colour composite (TCC) image generated using the red, green, blue bands and it has given contrast signature for anorthosite is a mixture of yellow and white colour. TCC is one of the combinations for anorthosite discrimination as it represents the true colour of an object as seen through the naked eye (Arivazhagan et al., 2017). The true colour composite image contains RGB (where R=Red, G=Green, and B=Blue) Bands, show shapes and sizes of features. The shape defines the geometric outline of an object. This outline gives information about the nature and geometry of the object. Size defines the magnitude of an object or a single dimension of the object (e.g., the length of a river) (Demirkesena et al., 2004).

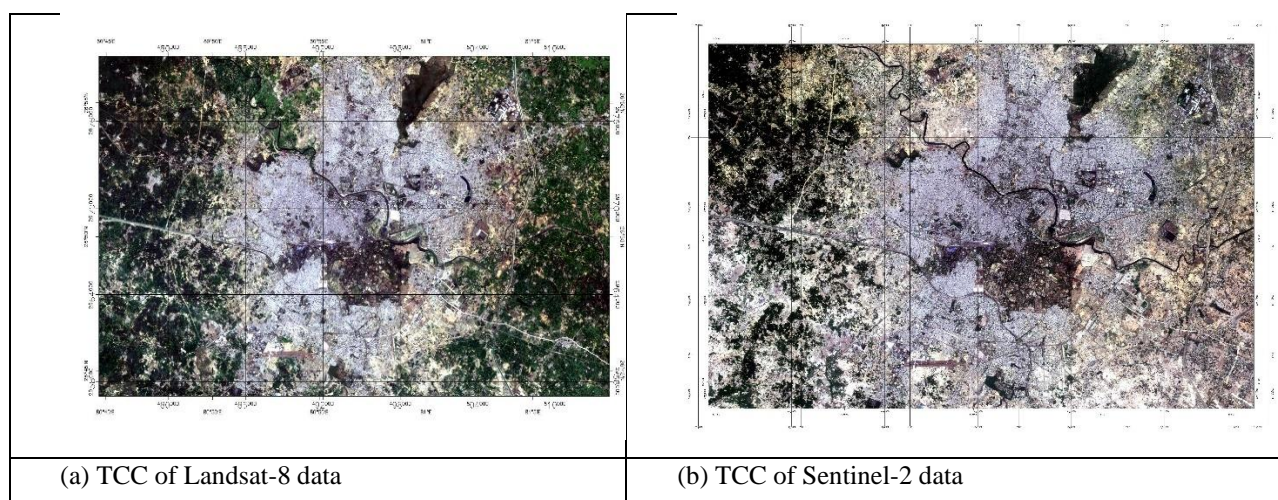


Figure.2 TCC image of Lucknow City (a) TCC of Landsat-8 data and (b) TCC of Sentinel-2 data.

3.2. Artificial Neural Network

Artificial neural networks are the computing model that is inspired by biological neural networks and provide new directions to solve problems arising in natural tasks (Sharma et al., 2013). A neuron receives inputs from a large number of other neurons or an external stimulus. Weighted sums of these inputs are fed into a nonlinear

activation function. The output of this function is distributed to connections of other neurons. The topology of neuron connections defines the flow of information in the network (Sharma et al., 2013).

Image similarity measurement is a fundamental problem in the field of computer vision, it is widely used in image classification, object detection, and image retrieval, etc. (Yuan et al., 2019). The objective of image similarity measurement is to estimate the given pair of the image are similar or not (Yuan et al., 2019). In the last few years, neural network models have been used extensively to solve machine learning problems/tasks (Yuan et al., 2019). Satellite images have been successfully applied in many applications such as classification, change detection, etc. satellite image processing involves some pre-processing procedure in classification and change detection approaches (Ma et al., 2019). In the neural network, many algorithms have been used by the remote sensing community for many years (Ma et al., 2019). The backpropagation based training of neural networks with multi-layers become an explicit research subject in the early 1990s but it was largely ignored by the machine learning community of that time (Ma et al., 2019). A neural network model is capable to learn a similarity measurement between two images/patterns, the similarity neural network architecture guarantees the basic properties of similarity measurement (Maggini et al., 2012). The similarity measurement is frequently used in a generic sense, describing both similarity and dissimilarity (Maggini et al., 2012). The analysis of the theoretical properties and approximation capabilities of SBNN is proven to universal approximation symmetric functions (Maggini et al., 2012).

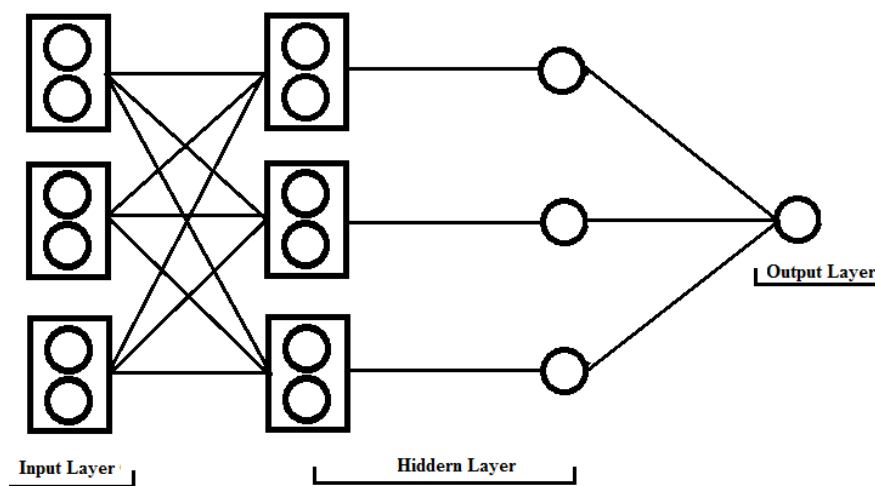


Figure.3 Block Diagram of Similarity-Based Neural Network Model

3.3.Color Feature

Image features are the visual content of an image, it can be described by colour, texture, and shape (Bunte et al., 2011). Image retrieval is the task of searching similar images of a certain type from an image repository. In recent years, the real-time application of image retrieval has gained great interest in the research area (Ahmed et al., 2019). Image retrieval has very popular research topic since the 1990s. Many researchers have used colour features to depict image features for region matching, semantic categorization, and similarity searches (Lu et al., 2007). Image feature extraction and analysis are significant research areas of computer vision (Wu et al., 2020). In the field of the image retrieval system, image features play an important role in image retrieval. (Bunte et al., 2011).

Colour images are the most significant parts of acknowledgement by people, and Color features are progressively utilized in image retrieval frameworks (Inbaraj et al., 2020). The colour feature is one of the basic features of the image (Huang et al., 2010). It is employed extensively because colour is an effective and robust visual cue for distinguishing one object from another (Xu et al., 2012). It contains three basic components in the image that are red, green, and blue, the colour feature can be obtained in the image based on pixel intensities (Sutojo et al., 2017). The colour components red, green, and blue are controlled independently, so every block has three mean values of pixel colours for the colour components red, green, and blue(Chan et al., 2004). The colour features fuse the colour distribution and spatial information of pixels in an image. The colour features can be extracted by using a simple and quick process (Chan et al., 2004). There are many methods such as colour histogram, colour correlogram, colour moment, colour structure descriptor, and scalable colour descriptor which are used to extract colour features from the image (Huang et al., 2010). The colour moment algorithm has the lowest feature vector dimension and lowers computational complexity so it is the most relevant method for image retrieval (Huang et al., 2010). In this study colour moment, an algorithm is used to extract colour features from the

image, the colour moment algorithm is used to calculate the standard deviation, and mean of each colour component of an image such as Red, Green, and Blue bands. The formula of mean and standard deviation are given below (Srivastava et al., 2021):

$$E_i = \sum_{j=1}^N \frac{1}{N} P_{ij} \quad (1)$$

$$\sigma_i = \sqrt{\frac{1}{N} \sum_{j=1}^N (P_{ij} - E_i)^2} \quad (2)$$

Where ‘i’ is the current channel index, ‘j’ is the number of channels. E_i is the mean (first moments) of the two image distributions and ‘ σ_i ’ is the standard deviation (second moments) of the two image distributions.

In this study, the colour moment algorithm is used to extract colour features from an image. Some of the extracted feature values are mention in Table 2.

Acquisition Date	Image ID	MeanR	MeanG	MeanB	StdR	StdG	StdB
06/28/2019	Img_1	133.49	128.72	128.7	68.457	66.237	66.533
04/29/2019	Img_2	138.81	128.15	128.65	66.367	65.473	64.634
01/21/2018	Img_3	115.5	122.24	131.43	67.72	64.092	67.794
12/23/2018	Img_4	122.32	127.3	132.49	62.031	60.347	62.922
02/09/2019	Img_5	106.74	107.85	105.36	72.657	68.968	71.079
06/17/2019	Img_6	137.06	133.9	137.67	65.14	63.315	63.896
03/13/2019	Img_7	107.33	105.07	108.58	71.158	70.61	73.369
03/29/2019	Img_8	116.65	114.81	119.1	67.733	68.577	70.462
12/10/2019	Img_9	142.42	146.5	141.6	61.635	60.222	61.313
01/27/2020	Img_10	113	122.84	120.41	67.287	62.006	67.606
02/12/2020	Img_11	108.79	112.55	111.45	68.308	65.01	70.365
04/16/2020	Img_12	132.73	122.24	124.09	63.657	63.867	63.016

Table.2. Colour Features of Sample Images Features of Sample Images

The steps required for colour feature extraction (Alsmadi et al., 2017):

1. The colour planes values red, green, blue are separated into individual matrices.
2. For each colour metric, a colour histogram is calculated.
3. Mean, and standard deviation of each colour histogram are calculated.
4. The calculated features of all metrics (red, green, and blue) are combined as a feature vector.
5. The feature vectors are stored in the feature database.

3.4.Minkowski Distance

The use of images is increasing all over the world, because it is capable of expressing, sharing, and interpreting information. While working with images, it is necessary to have the appropriate image of a particular situation (Yasmin et al., 2014). Feature-based image retrieval system uses the image features descriptors for image search and retrieval (MO et al., 2019). The purpose of the FBIR system is allowing to the user to retrieve images from the image repository (Herráez et al., 2008). An image is usually represented as a set of low-level descriptions (Herráez et al., 2008). The critical phase of the FBIR system is image feature extraction, image feature extraction techniques help to extract the hidden information from the image (Palwe et al., 2018). Feature-based searching is too easy when the system deals with tens of images but if the number of images is a hundred to thousand, the same task is extremely complex (Yasmin et al., 2014). A feature-based image retrieval system uses the image features descriptors for image search and retrieval (MO et al., 2019). The purpose of the FBIR system to allow the user that they can retrieve images from the image repository as per the study requirement (Herráez et al., 2008). An image is usually represented as a set of low-level descriptions (Herráez et al., 2008).

In this study, the Minkowski distance measurement algorithm is used to calculate the distance between query image features (a set of features that is return by feature database) and base image (referenced image) features. The Minkowski distance defines a distance between two points in a normed vector space and is a generalization of the Euclidean distance and the Manhattan distance. Minkowski distance between two variables X and Y is defined as (Malik et al., 2013)

$$\text{Distance}(x,y) = (\sum |X_i - Y_i|^p)^{1/p} \quad (3)$$

The Minkowski distance defines a distance between two points in a normed vector space. When $p=1$ then the distance is known as the Manhattan distance, when $p=2$ then the distance is known as the Euclidean distance (Malik et al., 2013). In the limit that $p \rightarrow +\infty$, the distance is known as the Chebyshev distance.

4. Model Development & Implementation

4.1. Development of SBNN based FBIR System

To retrieve the noise and cloud-free optical satellite images, there is a need for an intelligent satellite image retrieval system that always allows retrieving those images which are better for post-processing and also can produce an efficient result for interpretation and analysis of earth surface monitoring. Therefore, to fulfil this objective a feature-based image retrieval (FBIR) system has been developed, which uses the image features and similarity measurement technique to retrieve the best possible image from the repository. In our previous study (Srivastava et al., 2021), the k-nearest neighbours (KNN) algorithm based FBIR system was developed. The FBIR system has an image repository that contains the best possible images of every year. The images of the repository act as a referenced image in this system, and the selection of referenced images depends on the classification results as details are given in (Srivastava et al., 2021). The KNN algorithm calculates the overall similarity between images in the FBIR system. A satellite image holds multi-band data, and it is less capable to find similar bands between images so needs a model that is capable to calculate the similar bands between images. In the current study, the working process of the FBIR system is similar to our previous FBIR system (Srivastava et al., 2021) with a slight change. In order to develop an improved FBIR system, a similarity-based neural network (SBNN) has been used in place of the KNN algorithm. The SBNN is capable to find similar bands between images, and on the basis of band similarity, the system predicts that the image is suitable for post-processing or not. The complete working diagram of FBIR is shown in figure 4.

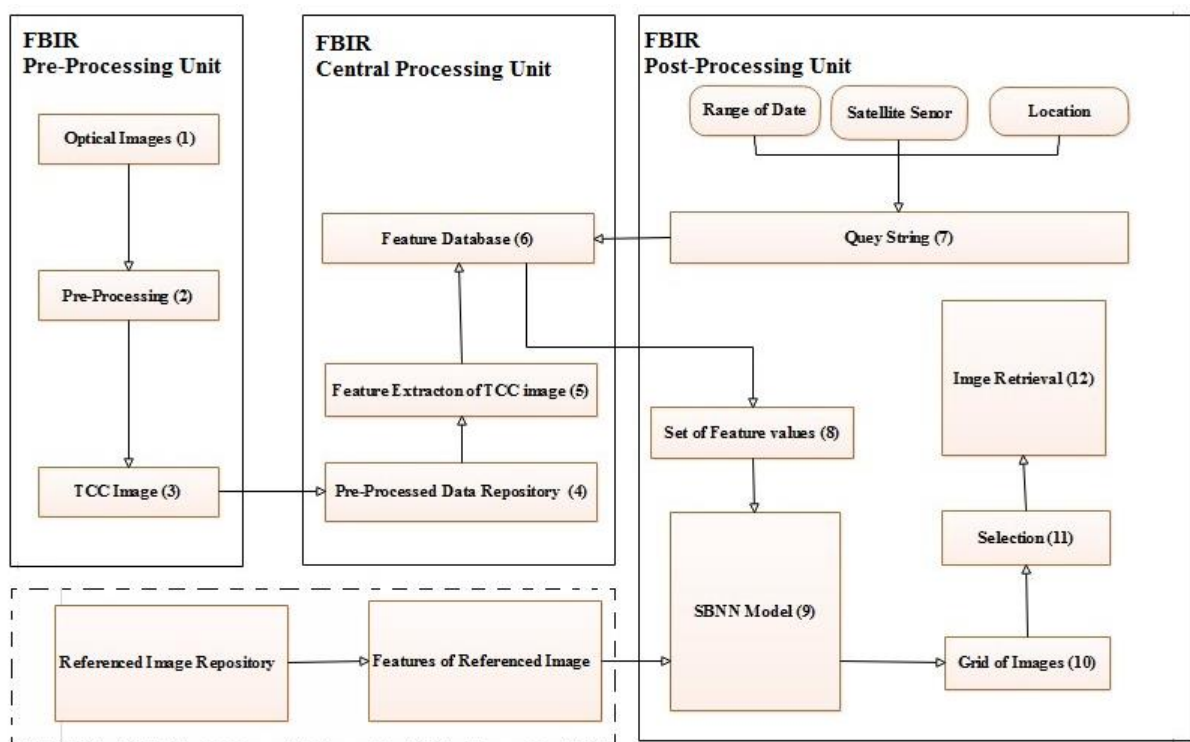


Figure.4 Working diagram of SBNN based FBI System

The FBIR system consists of three major units a pre-processing unit, a central processing unit, and the post-processing unit, and each unit of the system contains a unique responsibility as described in (Srivastava et al., 2021). The SBNN model is capable to identify those satellite images which are similar or not by using the image features. In SBNN, at least two satellite images are required first is a query image (a set of features that is extracted from the database) and the second one is a base image (a referenced image from Referenced Image Repository). The SBNN model matches the features of the query image with the base image, and based on the similarity of the feature, the model predicts that images are assessed. Image matching between query image features and base image features is done by using distance metrics. The distance vector with a small value defines the deep similarity between them (Malik et al., 2013). The flow chart of the developed SBNN model is shown in figure 5.

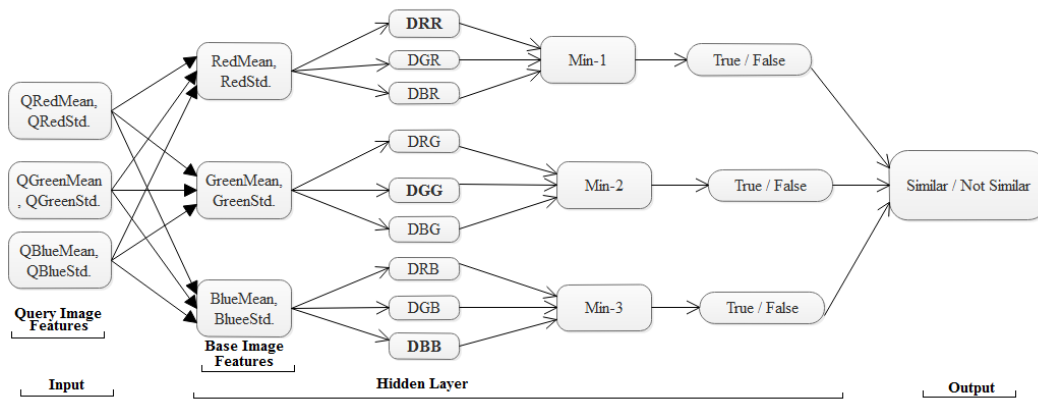


Figure.5 Similarity-Based Neural Network Model

In Fig. 5, all features of query image interact with features of base image one by one and calculate the band similarity between them using a distance measurement algorithm, and based on band similarity, the model assessed the image.

4.2. Implementation of SBNN based FBIR System

Image matching is a crucial task of any FBIR system; the SBNN model is capable to find the similarity between two or more satellite images. For feature matching, at least two images are required, the first one acts as a query image, and the second one-act as a base image (i.e. Referenced image). The colour moment algorithm has been used to extract colour features from the TCC image of both images, and the extracted values need to store in a multidimensional array. The counter array needs to be created so that it will contain TRUE, and FALSE value based on the similarity between patterns of the query image. A stepwise implementation of SBNN based FBIR model is followed as:

4.2.1. Similarity Measurement with Red Band of Base image

In this step, all the features of query image like QReadMean, QRedStd, QGreenMean, QGreenStd, QBlueMean, and QBlueStd were mapped with Red features of the base image (i.e. ReadMean and RedStd), and calculate the minimum distance between them as shown in Figure 6.

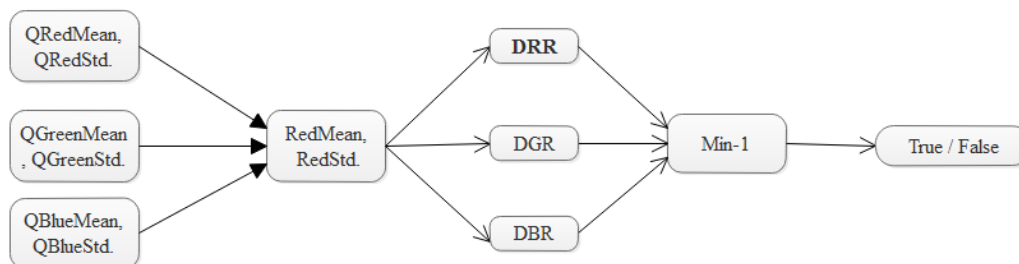


Figure.6 Query Image Features interacts with Red Features of Base Image

After the completion of this phase, three different value received as the distance between Red features of the query image and Red features of the base image (DRR), the distance between Green features of the query image and Red features of the base image (DGR), and distance between Blue features of the query image and Red features of the base image (DBR). Now, SBNN finds out the minimum distance value among them (Min-1), if DRR consists of minimum value means red features of the query image are deeply-nearest with the Red features of the base image means Red features of both images are similar so TRUE was assigned on the first index of the counter array, otherwise FALSE was assigned.

4.2.2. Similarity Measurement with Green Band of Base image

In this step, All the features of query image like QReadMean, QRedStd, QGreenMean, QGreenStd, QBlueMean, and QBlueStd were mapped with green features of the base image (i.e. GreenMean and GreenStd), and estimate the minimum distance between them as shown in Figure 7.

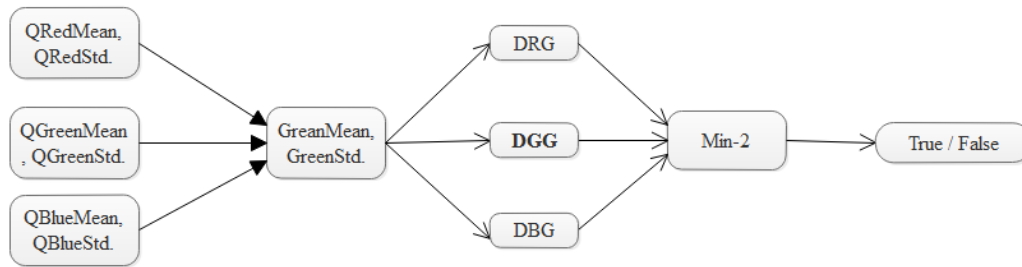


Figure.7 Query Image Features interacts with Green Features of Base Image

In this phase, three different value received as the distance between Red features of the query image and Green features of the base image (DRG), the distance between Green features of the query image and Green features of the base image (DGG), and distance between Blue features of the query image and Green features of the base image (DBG). Now, SBNN finds out the minimum distance value among them (Min-2), if DGG consists minimum value means green features of the query image are deeply-nearest with the green features of the base image means green features of both images are similar so TRUE was assigned on the second index of the counter array, otherwise FALSE was assigned.

4.2.3.Measurement with Blue Band of Base image

In this step, all the features of query image such as QReadMean, QRedStd, QGreenMean, QGreenStd, QBlueMean, and QBlueStd were mapped with Blue features of the base image (i.e. BlueMean, and BlueStd), and compute the minimum distance between them as shown in Figure 8.

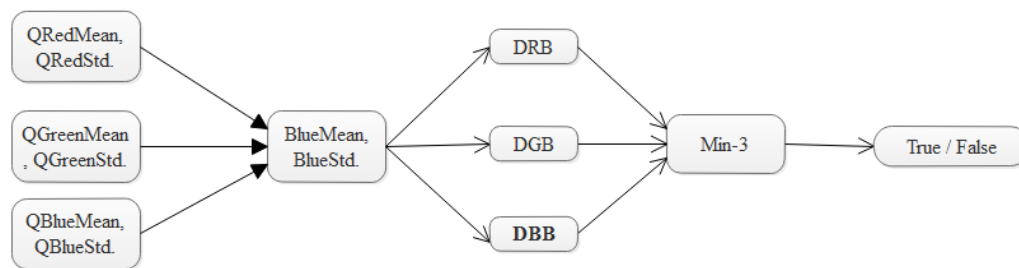


Figure.8 Query Image Features interacts with Blue Features of Base Image

After the computation of similarity with the Blue band of the query image, three different value received as the distance between Red features of the query image and Blue features of the base image (DRB), the distance between Green features of the query image and Blue features of the base image (DGB), and distance between Blue features of the query image and Blue features of the base image (DBB). Now, SBNN finds out the minimum distance value among them (Min-3), if DBB consists minimum value means Blue features of the query image are deeply-nearest with Blue features of the base image means Blue features of both images are similar so TRUE was assigned on the third index of the counter array, otherwise FALSE was assigned on the third index of the counter array.

4.2.4.Prediction of Image Quality Assessment

The counter array plays an important role in this model, the number of TRUE elements in an array decides the quality of images. In this step, If the counter array consists of three TRUE values means the image is perfectly similar and if the counter array does not contain a TRUE value means images are not similar as shown in Figure 9.

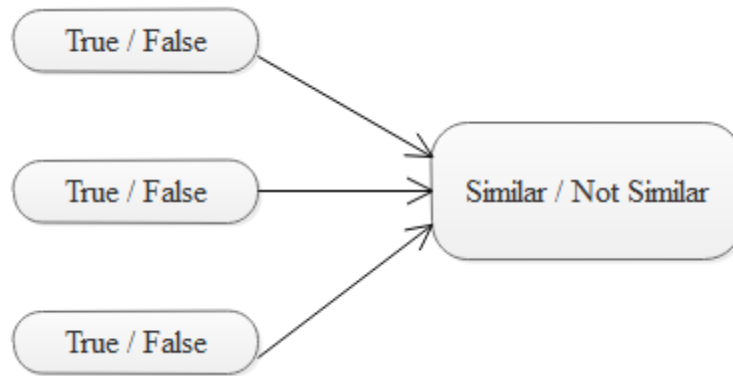


Figure.9 Prediction phase of SBNN Model

5. Results and Discussions

The critical problem of a feature-based image retrieval system is to find similar images in the repository. In this study, develop a similarity-based neural network model that is capable to find similarities between. The SBNN model matches the similarity between query image and base image, and predict that images are similar or not using the similarity result. In the initial phase of the SBNN model development, multiple optical satellite images (i.e. Landsat-8 OLI, and Sentinel 2) were collected and pre-processed to build an offline image repository. The image repository contains approximately 140 satellite images from February 17, 2016, to April 16, 2020, which were pre-processed one by one and stored in the Pre-processed image repository.

Two Landsat-8 OLI images of 27 January 2020 (Img ID: IMG_10) and 16 April 2020 (Image ID: IMG_12) as given in Table 1, have been used for the development of the SBNN model for the FBIR System. In the pre-processing phase, radiometric calibration has been applied on each Landsat image which is stored in the image repository to convert the digital number of an image into surface reflectance values. After pre-processing on all the images, the area of interest (study area) has been cropped from images and then true colour composite (TCC) images have been generated one by one using the Red, Green, and Blue bands, and generated TCC images are stored in the Pre-processed Image Repository. TCC images generated through Img_10 and Img_12 are shown in Figure 10 (a) and 10 (b) and color histogram of IMG_10 and IMG_12 are shown in Figure 11 (a) and 11 (b).

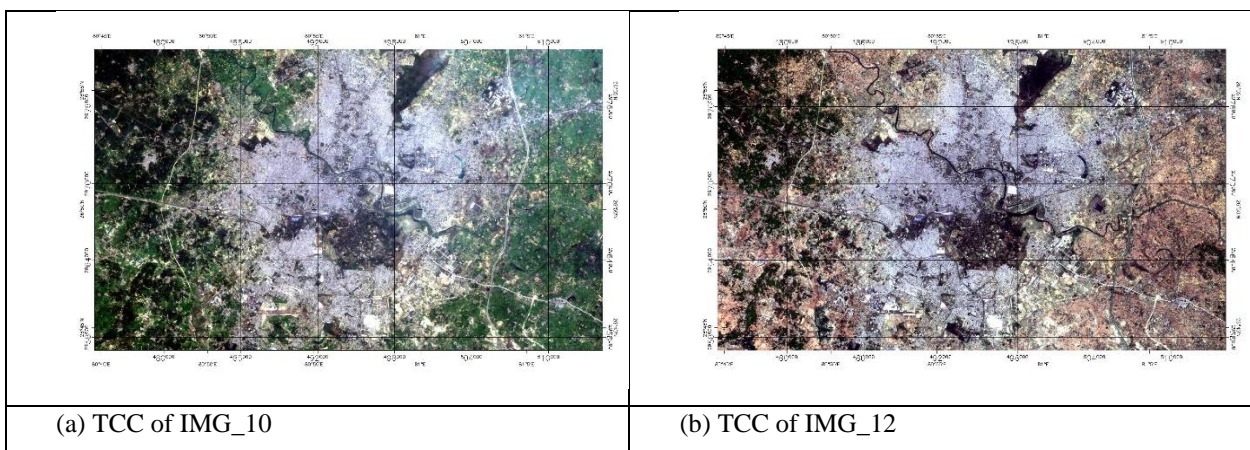


Figure.10 TCC image of the study area (a) TCC of IMG_10 and (b) TCC of IMG_12

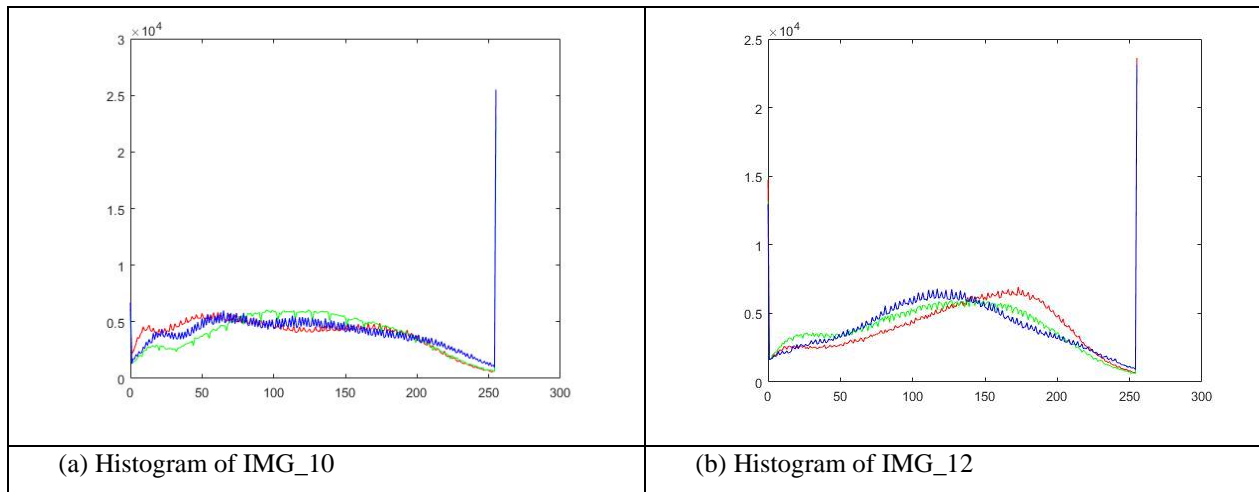


Figure.11 Color histogram of study area (a) IMG_10 and (b) IMG_12

In this study, the colour moment algorithm is used to extract colour features from an image. Color features of *Img_10* and *Img_12* are mention in Table 3.

Sr No.	Image ID	MeanR	MeanG	MeanB	StdR	StdG	StdB
1	IMG_10	113	122.84	120.41	67.287	62.006	67.606
2	IMG_12	132.73	122.24	124.09	63.657	63.867	63.016

Table.3. Color Features of *Img_10* and *Img_12*

Similarly, the colour moment algorithm is applied on all images and the retrieved feature values like MeanR, MeanG, MeanB, StdR, StdG, and StdB of Red, Green, and Blue bands are stored in the feature database as shown in Figure 12.

Data	Acquisition_ID	Acquisition_Date	Tcc	Location	State	Country	top_left_lat	top_left_lon	bottom_right_lat	bottom_right_lon	MeanR	MeanG	MeanB	stdR	stdG	stdB
Landsat-8	LC08_L1TP_144041_20191023_20191030_01_T1	2019-10-23	tcc/23oct2019	Lucknow	Uttar Pradesh	India	26.9457497	80.7445117	26.7348307	81.1425887	78.999	78.199	78.316	65.501	65.444	65.671
Landsat-8	LC08_L1TP_144041_20191108_20191115_01_T1	2019-11-08	tcc/8nov2019	Lucknow	Uttar Pradesh	India	26.9457497	80.7445117	26.7348307	81.1425887	115.75	109.54	100.2	56.479	51.088	49.667
Landsat-8	LC08_L1TP_144041_20191124_20191203_01_T1	2019-11-24	tcc/24nov2019	Lucknow	Uttar Pradesh	India	26.9457497	80.7445117	26.7348307	81.1425887	147.51	149.14	143.13	58.915	58.975	57.243
Landsat-8	LC08_L1TP_144041_20191210_20191217_01_T1	2019-12-10	tcc/10dec2019	Lucknow	Uttar Pradesh	India	26.9457497	80.7445117	26.7348307	81.1425887	142.42	148.5	141.6	61.835	60.222	61.313
Landsat-8	LC08_L1GT_144041_20191228_20200110_01_T2	2019-12-28	tcc/28dec2019	Lucknow	Uttar Pradesh	India	26.9457497	80.7445117	26.7348307	81.1425887	149.24	149.97	152.26	55.727	55.626	55.628
Landsat-8	LC08_L1TP_144041_20200111_20200114_01_T1	2020-01-11	tcc/11jan2020	Lucknow	Uttar Pradesh	India	26.9457497	80.7445117	26.7348307	81.1425887	158.55	158.8	161.67	53.665	53.942	54.371
Landsat-8	LC08_L1TP_144041_20200127_20200210_01_T1	2020-01-27	tcc/27jan2020	Lucknow	Uttar Pradesh	India	26.9457497	80.7445117	26.7348307	81.1425887	113	122.84	120.41	67.287	62.006	67.606
Landsat-8	LC08_L1TP_144041_20200212_20200225_01_T1	2020-02-12	tcc/12feb2020	Lucknow	Uttar Pradesh	India	26.9457497	80.7445117	26.7348307	81.1425887	108.79	112.55	111.45	68.308	65.01	70.365
Landsat-8	LC08_L1TP_144041_20200315_20200325_01_T1	2020-02-28	tcc/28feb2020	Lucknow	Uttar Pradesh	India	26.9457497	80.7445117	26.7348307	81.1425887	76.93	74.159	72.956	69.888	70.382	70.72
Landsat-8	LC08_L1TP_144041_20200228_20200313_01_T1	2020-03-15	tcc/15march2020	Lucknow	Uttar Pradesh	India	26.9457497	80.7445117	26.7348307	81.1425887	82.53	76.628	67.991	56.144	49.696	48.975
Landsat-8	LC08_L1TP_144041_20200331_20200410_01_T1	2020-03-31	tcc/31march2020	Lucknow	Uttar Pradesh	India	26.9457497	80.7445117	26.7348307	81.1425887	108.55	103.92	102.25	64.575	66.467	68.786
Landsat-8	LC08_L1TP_144041_20200416_20200418_01_RT	2020-04-16	tcc/16april2020	Lucknow	Uttar Pradesh	India	26.9457497	80.7445117	26.7348307	81.1425887	132.73	122.24	124.09	63.657	63.867	63.016
Landsat-8	LC08_L1TP_144041_20181105_20181115_01_T1	2018-11-05	tcc/5Nov2018	Lucknow	Uttar Pradesh	India	26.9457497	80.7445117	26.7348307	81.1425887	130.7	127.76	124.19	63.646	63.488	64.649
Landsat-8	LC08_L1GT_144041_20181016_20181018_01_T2	2018-01-05	tcc/5Jan2018	Lucknow	Uttar Pradesh	India	26.9457497	80.7445117	26.7348307	81.1425887	138.89	139.93	141.56	57.883	57.714	57.774
Landsat-8	LC08_L1TP_144041_20181207_20181211_01_T1	2018-12-07	tcc/7Dec2018	Lucknow	Uttar Pradesh	India	26.9457497	80.7445117	26.7348307	81.1425887	129.37	134.09	137.97	60.983	60.26	61.043
Landsat-8	LC08_L1TP_144041_20180411_20180417_01_T1	2018-04-11	tcc/11Apr2018	Lucknow	Uttar Pradesh	India	26.9457497	80.7445117	26.7348307	81.1425887	166.35	165.88	166.6	50.888	50.884	51.379
Landsat-8	LC08_L1TP_144041_20180513_20180517_01_T1	2018-05-13	tcc/13May2018	Lucknow	Uttar Pradesh	India	26.9457497	80.7445117	26.7348307	81.1425887	137.53	138.23	144.25	63.531	62.409	63.705
Landsat-8	LC08_L1TP_144041_20180614_20180703_01_T1	2018-06-14	tcc/14June2018	Lucknow	Uttar Pradesh	India	26.9457497	80.7445117	26.7348307	81.1425887	153.85	152.41	153.6	54.324	55.226	57.213
Landsat-8	LC08_L1TP_144041_20180121_20180206_01_T1	2018-01-21	tcc/21Jan2018	Lucknow	Uttar Pradesh	India	26.9457497	80.7445117	26.7348307	81.1425887	115.5	122.24	131.43	67.72	64.092	67.794
Landsat-8	LC08_L1TP_144041_20181121_20181121_01_RT	2018-11-21	tcc/21Nov2018	Lucknow	Uttar Pradesh	India	26.9457497	80.7445117	26.7348307	81.1425887	134.83	137.05	143.77	61.272	60.712	60.731
Landsat-8	LC08_L1TP_144041_20180222_20180308_01_T1	2018-02-22	tcc/22Feb2018	Lucknow	Uttar Pradesh	India	26.9457497	80.7445117	26.7348307	81.1425887	112.72	115.06	123.06	68.898	68.027	68.693
Landsat-8	LC08_L1TP_144041_20180427_20180502_01_T1	2018-04-27	tcc/27Apr2018	Lucknow	Uttar Pradesh	India	26.9457497	80.7445117	26.7348307	81.1425887	137.37	136.6	138.22	63.271	63.056	64.262
Landsat-8	LC08_L1TP_144041_20180529_20180605_01_T1	2018-05-29	tcc/29May2018	Lucknow	Uttar Pradesh	India	26.9457497	80.7445117	26.7348307	81.1425887	135.01	135.18	141.24	64.293	62.625	64.896
Landsat-8	LC08_L1TP_144041_20180716_20180730_01_T1	2018-07-16	tcc/16July2018	Lucknow	Uttar Pradesh	India	26.9457497	80.7445117	26.7348307	81.1425887	63.07	59.83	55.721	63.782	64.555	65.697
Landsat-8	LC08_L1GT_144041_20180801_20180814_01_T2	2018-08-01	tcc/1Aug2018	Lucknow	Uttar Pradesh	India	26.9457497	80.7445117	26.7348307	81.1425887	120.55	120.53	121.71	63.917	64.014	64.488
Landsat-8	LC08_L1TP_144041_20180817_20180829_01_T1	2018-08-17	tcc/17Aug2018	Lucknow	Uttar Pradesh	India	26.9457497	80.7445117	26.7348307	81.1425887	72.818	74.271	71.88	57.894	57.299	56.155

Figure.12 Color Features of Images (Feature Database)

A web portal (i.e. a graphical user interface (GUI)) had been developed for the FBIR system to retrieve the best possible image from the image repository. The user gives a query string as an input, the system aligns the best possible images based on the query string in the form of a grid. The user selects an image from the grid, and the system serves it as a result. The query string is a combination of a range of acquisition dates (start_date and end_date), the name of the satellite sensor, and the location of the required image. The developed GUI for FBIR is shown in Figure 13 (which is available at <http://newfbirsystem.asaptechnosystems.com>) in which the user gives a query string as input in the system. The FBIR system receives a query string as input and forwards it to the feature database, the feature database returns a set of features values according to a query string, each set of features interacts with the best possible image of that year (referenced image) one by one, and calculate the similarity

using distance measurement technique and based on similarity score, the system predicts that image is good for post-processing or not.

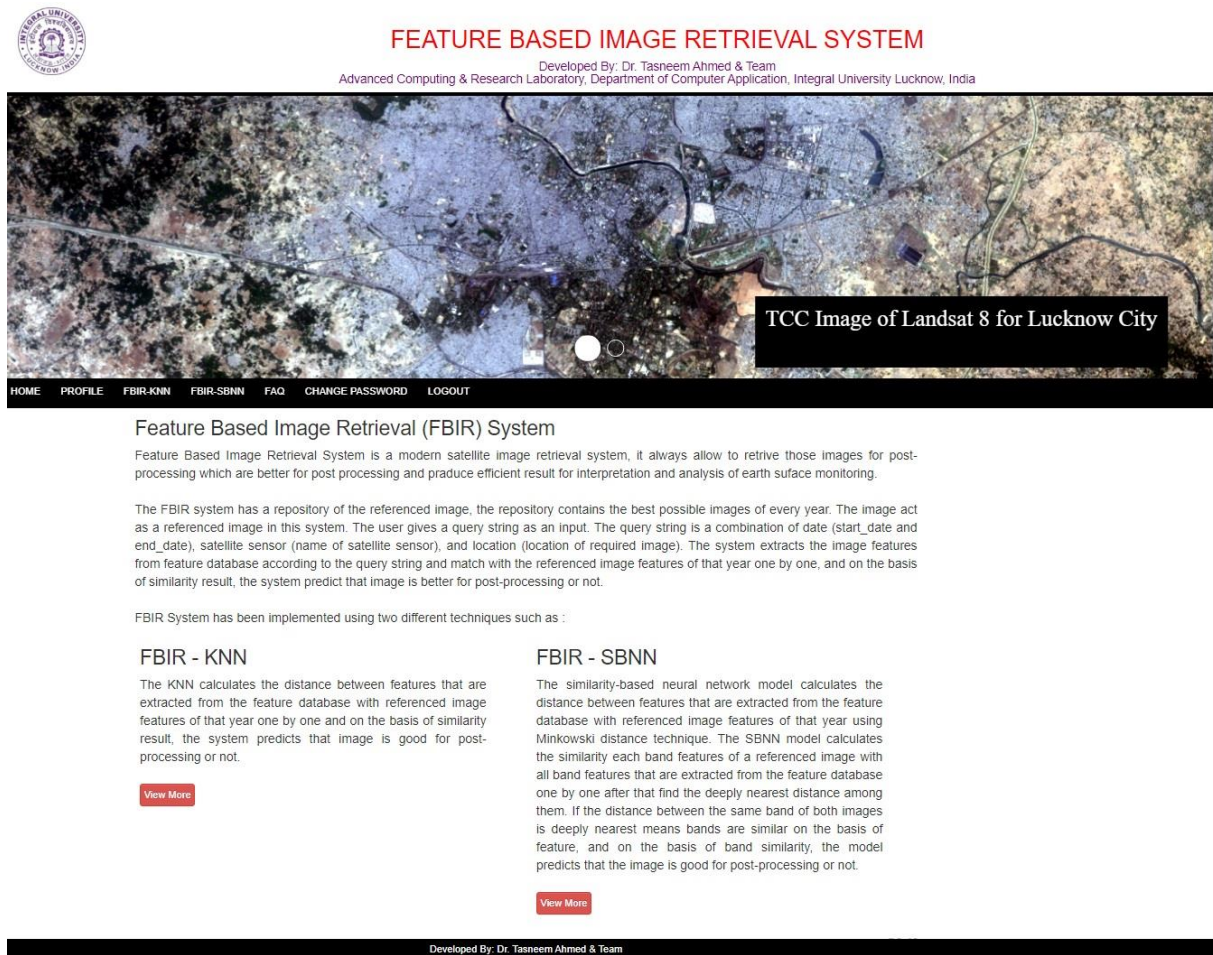


Figure.13 GUI- feature-based image retrieval (FBIR) system

The similarity-based neural network model of the FBIR system calculates the distance between features that are extracted from the feature database with referenced image features of that year using the Minkowski distance technique. The SBNN model calculates the similarity of each band feature of a referenced image with all band features of a set of features that are extracted from the feature database, after that find the minimum distance value (deeply nearest distance) among them. If the distance between the same band of both images is deeply nearest means bands are similar based on features and based on band similarity band, the model predicts that the image is good for post-processing or not. The property of interpretation of band similarity mention in Table 4.

Sr No.	Band Similarity	Properly
1	Three	Perfectly similar, and best for post-processing.
2	Two	Partial similar, and good for post-processing.
3	One	Partial similar, and okay for post-processing.
4	Zero	Not similar

Table.4. property of interpretation of similarity score.

The value of p plays an important role in the similarity measurement task to determine how close the result will be.

Suppose, two objects are $X = [2, 3]$ and $Y = [4, 5]$, and now calculate the distance between X and Y using the Minkowski algorithm with $p = 1, 2, 3, 4, \text{ and } 5$. We will put the value of p in eqn(3), and obtain a new formula for distance measurement. The distance between two objects will never be negative. Mathematical formulation and expected results are mention in Table 5.

Sr No.	p	Formula	Calculation	Result
1	1	Distance $(x,y)=(\sum Xi-Yi ^1)^{1/1}$	$((2-4)^1+(3-5)^1)^{1/1}$	4
2	2	Distance $(x,y)=(\sum Xi-Yi ^2)^{1/2}$	$((2-4)^2+(3-5)^2)^{1/2}$	2.82
3	3	Distance $(x,y)=(\sum Xi-Yi ^3)^{1/3}$	$((2-4)^3+(3-5)^3)^{1/3}$	2.51
4	4	Distance $(x,y)=(\sum Xi-Yi ^4)^{1/4}$	$((2-4)^4+(3-5)^4)^{1/4}$	2.37
5	5	$(x,y)=(\sum Xi-Yi ^5)^{1/5}$	$((2-4)^5+(3-5)^5)^{1/5}$	2.2

Table.5. distance between two objects by Minkowski Algorithm.

From table 5, the value of p playing an important role to calculate the distance between two objects, the distance value with a small number defines the deep similarity between them. The way in which the value of p is increasing, getting closer to the result. Hence in this study, p=5 has been used with the Minkowski distance measurement algorithm for finding deeply-nearest results, and the new formula of similarity measurement in this study is given below:

$$\text{Distance } (x,y)=(\sum|Xi-Yi|^5)^{1/5}$$

The reference image of that year (2020) helps to find better images from the set of feature values returned by the feature database. The SBNN model calculates the similarity bands between referenced image and a set of feature values, and on the basis of the similarity band, the system predicts that the image is suitable for post-processing or not. In the development phase, IMG_10 acts as a referenced image, and IMG_12 acts as a set of feature values (Query Image). The SBNN model matches the query image features with referenced image features through four major steps.

Step 1: Similarity Measurement with Red Band of Base image

All set of image features of Img_12 are mapped with Red features of the referenced image (i.e. Img_10) and computed the distance between them, and if Red band features of both images are deeply nearest then assign TRUE in remark otherwise assign FALSE as mentioned in table 6.

Band	Img_12		Img_10		Distance	Remark
	Mean	Std. Dev.	Red Mean	Red Std. Dev.		
Red	132.73	63.657	113	67.287	19.73	FALSE
Green	122.24	63.867			9.89	
Blue	124.09	63.016			12.32	

Table.6. Matching of Red, Green, and Blue Features of Img_12 with Red feature of Img_10 image

From Table 6, it is observed that the distance between Red band features of both images is not deeply nearest because the distance value of it is not minimum to compare than other distance value hence assigned FALSE in a remark.

Step 2: Similarity Measurement with Green Band of Base image

All set of image features of Img_12 are mapped with Green features of the referenced image (i.e. Img_10) and calculated the distance between them, and if green band features of both images are deeply nearest then assign TRUE in remark otherwise assign FALSE as mentioned in table 7.

Band	Img_12		Img_10		Distance	Remark
	Mean	Std. Dev.	Green Mean	Green Std. Dev.		
Red	132.73	63.657	122.84	62.006	9.25	TRUE
Green	122.24	63.867			1.86	
Blue	124.09	63.016			3.75	

Table.7. Matching of Red, Green, and Blue Features of Img_12 with Green feature of Img_10 image

From Table 7, it is observed that the distance between green band features of both images is deeply nearest because the distance value of it is minimum to compare than other distance value hence assigned TRUE in a remark.

Step 3: Similarity Measurement with Blue Band of Base image

All set of image features of Img_12 are mapped with Blue features of the referenced image (i.e. Img_10) and estimated the distance between them, and if Blue band features of both images are deeply nearest then assign TRUE in remark otherwise assign FALSE as mentioned in table 8.

Band	Img_12		Img_10		Distance	Remark
	Mean	Std. Dev.	Blue Mean	Blue Std. Dev.		
Red	132.73	63.657	120.41	67.606	11.10	FALSE
Green	122.24	63.867			1.32	
Blue	124.09	63.016			4.86	

Table.8. Matching of Red, Green, and Blue Features of Img_12 with Blue feature of Img_10 image

From Table 8, it is observed that the distance between blue band features of both images is not deeply nearest because the distance value of it is not minimum to compare than other distance values hence assigned FALSE in a remark.

Step 4: Prediction of Image Quality Assessment

Observed that from table 6-8, Red and Blue band features of Img_12 image is not deeply-nearest with Red and Blue band features of Img_10 image but the green band features of both the images are deeply nearest hence it proves that one band of Img_12 image are nearest with Img_10 image so the image would partial similar, and okay for post-processing. After the analysis of similarity bands, the portal of the FBIR system will list all the best available images in the image grid and the system will suggest downloading only those images whose similarity band score is more than one as shown in Figure 14.




ACQUISITION DATE	RGB IMAGE	QUALITY ASSESSMENT	DOWNLOAD
2020-04-16		partial Similar, and okay for post-processing.	<input type="button" value="DOWNLOAD"/>
2020-03-31		partial Similar, and okay for post-processing.	<input type="button" value="DOWNLOAD"/>
2020-03-15		partial Similar, and okay for post-processing.	<input type="button" value="DOWNLOAD"/>

Figure.14 GUI- Grid of Images.

After clicking on the download button, the portal will be redirected to the final download page and will ask to select the pre-processed individual band data for download. Here, the user will be allowed to choose the required band image with Radiance/Reflectance/Brightness temperature as shown in Figure 15.

Date : 2020-04-16
Satellite sensor : Landsat-8

Landsat-8 Bands	Description	Wavelength	Resolution (m)	Download
Band 1	Coastal / Aerosol	0.433 to 0.453 μm	30 meter	Reflectance <input type="checkbox"/> Radiance <input type="checkbox"/>
Band 2	Visible blue	0.450 to 0.515 μm	30 meter	Reflectance <input type="checkbox"/> Radiance <input type="checkbox"/>
Band 3	Visible green	0.525 to 0.600 μm	30 meter	Reflectance <input type="checkbox"/> Radiance <input type="checkbox"/>
Band 4	Visible red	0.630 to 0.680 μm	30 meter	Reflectance <input type="checkbox"/> Radiance <input type="checkbox"/>
Band 5	Near-infrared	0.845 to 0.885 μm	30 meter	Reflectance <input type="checkbox"/> Radiance <input type="checkbox"/>
Band 6	Short wavelength infrared	1.56 to 1.66 μm	30 meter	Reflectance <input type="checkbox"/> Radiance <input type="checkbox"/>
Band 7	Short wavelength infrared	2.10 to 2.30 μm	60 meter	Reflectance <input type="checkbox"/> Radiance <input type="checkbox"/>
Band 8	Panchromatic	0.50 to 0.68 μm	15 meter	Reflectance <input type="checkbox"/> Radiance <input type="checkbox"/>
Band 9	Cirrus	1.36 to 1.39 μm	30 meter	Reflectance <input type="checkbox"/> Radiance <input type="checkbox"/>
Band 10	Long-wavelength infrared	10.3 to 11.3 μm	100 meter	Radiance <input type="checkbox"/> Brightness Temperature <input type="checkbox"/>
Band 11	Long-wavelength infrared	11.5 to 12.5 μm	100 meter	Radiance <input type="checkbox"/> Brightness Temperature <input type="checkbox"/>

Figure.15 List of images available for download

End-user can easily select the individual band image in Radiance/Reflectance/Brightness temperature as per their scientific study requirements, which will help to conduct a quick study for agriculture monitoring, flood monitoring, urban heat monitoring, yield prediction and coal fire monitoring.

5.1. Testing & Validation of SBNN based FBIR System

Testing and validation of the developed system are an important part, hence, to test and validate the developed SBNN based FBIR system two Sentinel-2 images of 28 June 2019 (Image ID: Img_1) and 29 April 2019 (Image ID: Img_2) as details are given in Table 1, have been utilized. In the pre-processing phase of Sentinel 2 resampling of the image are done. In this study, the B2 band is used to resampling the images and the spatial resolution of the B2 band is 10 meters. After resampling of all images, the area of interest has been cropped from these images and then true colour composite (TCC) images have been generated one by one using the Red, Green, and Blue bands, and generated TCC images are stored in the pre-processed image repository. TCC images generated through Img_1 and Img_2 are shown in Figure 16 (a) and 16 (b) and color histogram of Img_1 and Img_2 are shown in Figure 17 (a) and 17 (b).

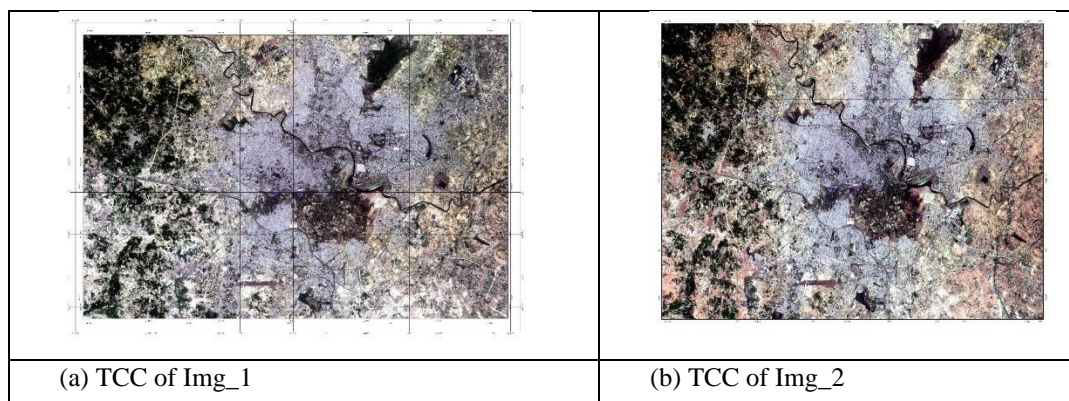


Figure.16 TCC image of study area (a) Img_1 and (b) Img_2

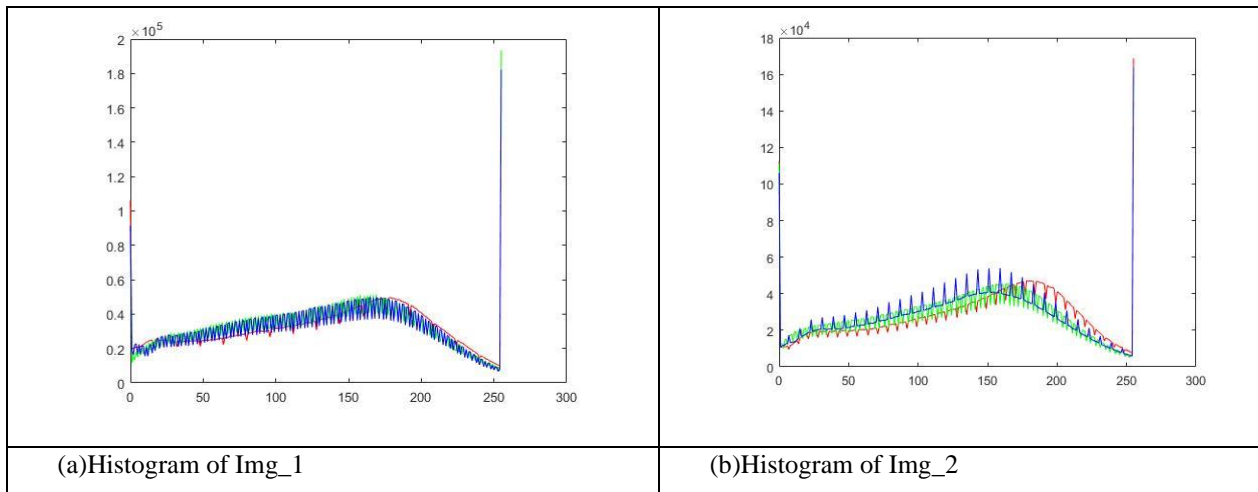


Figure.17 Color Histogram of study area (a) Img_1 and (b) Img_2

The extracted colour features of Img_1 and Img_2 are mention in Table 9.

Sr No.	Image ID	MeanR	MeanG	MeanB	StdR	StdG	StdB
1	Img_1	133.49	128.72	128.7	68.457	66.237	66.533
2	Img_2	138.81	128.15	128.65	66.367	65.473	64.634

Table.9. Color Features of Img_1 and Img_2

The referenced image (Img_1) of the input year (2019) helps to find the better image from the set of feature values of images that are returned by the feature database.

Step 1: Similarity Measurement with Red Band of Base image

All set of features (Img_2) mapped with Red features of the referenced image (Img_1) and distance between them calculated, and if Red band features of both images are deeply nearest then TRUE was assigned in remark otherwise FALSE was assigned as mentioned in table 10.

Band	IMG_2		IMG_1		Distance	Remark
	Mean	Std. Dev.	Red Mean	Red Std. Dev.		
Red	138.81	66.367	133.49	68.457	5.32	TRUE
Green	128.15	65.473			10.09	
Blue	128.65	64.634			10.11	

Table.10. Matching of Red, Green, and Blue Features of Img_2 image with Red feature of Img_1 image.

From Table 10, observed that the distance between the red band features of both images is deeply nearest because the distance value of it is minimum to compare than other distance value hence assigned TRUE in a remark.

Step 2: Similarity Measurement with Green Band of Base image

All set of features (Img_2) mapped with Green features of the referenced image (Img_1) and the distance between them were computed, and if Green band features of both images are deeply nearest then TRUE was assigned in remark otherwise FALSE was assigned as mentioned in table 11.

Band	IMG_2		IMG_1		Distance	Remark
	Mean	Std. Dev.	Green Mean	Green Std. Dev.		
Red	138.81	66.367	128.72	66.237	5.39	TRUE
Green	128.15	65.473			0.79	
Blue	128.65	64.634			1.06	

Table.11. Matching of Red, Green, and Blue Features of Img_2 image with Green feature of Img_1 image.

From Table 11, observed that the distance between the green band features of both images is deeply nearest because the distance value of it is minimum to compare than other distance value hence assigned TRUE in the remark.

Step 3: Similarity Measurement with Blue Band of Base image

All set of features (Img_2) mapped with Blue features of the referenced image (Img_1) and the distance was estimated between them, and if Blue band features of both images are deeply nearest then TRUE was assigned in remark otherwise FALSE was assigned as mentioned in table 12.

Band	Img_2		Img_1		Distance	Remark
	Mean	Std. Dev.	Blue Mean	Blue Std. Dev.		
Red	138.81	66.367	128.7	66.533	5.10	FALSE
Green	128.15	65.473			1.60	
Blue	128.65	64.634			1.89	

Table.12. Matching of Red, Green, and Blue Features of Img_2 image with the Blue feature of Img_1 image.

From Table 12, observed that the distance between the blue band features of both images is not deeply nearest because the distance value of it is not minimum to compare than other distance value hence assigned FALSE in a remark.

Step 4: Prediction of Image Quality Assessment

From table 10-12, it is observed that Red and Green band features of Img_2 image are deeply nearest with Red and Green band features of Img_1 image but the Blue band features of both images are not deeply nearest hence it proves that two bands of Img_2 image are nearest with Img_1 image so the image would partial similar, and good for post-processing.

The FBIR system will list all the best available images in the image grid and the system will suggest downloading only those images whose similarity bands are more than one as shown in Figure 18.



ACQUISITION DATE	RGB IMAGE	QUALITY ASSESSMENT	DOWNLOAD
2019-06-28		Perfectly Similar, and better for post-processing.	<input type="button" value="DOWNLOAD"/>
2019-05-24		Similar, and good for post-processing.	<input type="button" value="DOWNLOAD"/>

Figure.18 GUI- Grid of Images (Validation Phase)

After clicking on the download button, the portal will be redirected to the final download page and will ask for the final confirmation for the download.

Date : 2019-05-24
Satellite sensor : Sentinel-2

Sentinel-2 Bands	Wavelength (µm)	Resolution (m)	Download
Band 1 - Coastal aerosol	0.443	60	<input type="checkbox"/>
Band 2 - Blue	0.490	10	<input type="checkbox"/>
Band 3 - Green	0.560	10	<input type="checkbox"/>
Band 4 - Red	0.665	10	<input type="checkbox"/>
Band 5 - Vegetation Red Edge	0.705	20	<input type="checkbox"/>
Band 6 - Vegetation Red Edge	0.740	20	<input type="checkbox"/>
Band 7 - Vegetation Red Edge	0.783	20	<input type="checkbox"/>
Band 8 - NIR	0.842	10	<input type="checkbox"/>
Band 8A - Vegetation Red Edge	0.865	20	<input type="checkbox"/>
Band 9 - Water vapour	0.945	60	<input type="checkbox"/>
Band 10 - SWIR - Cirrus	1.375	60	<input type="checkbox"/>
Band 11 - SWIR	1.610	20	<input type="checkbox"/>
Band 12 - SWIR	2.190	20	<input type="checkbox"/>

Figure.19 Fig 25. GUI- Image Retrieval (Validation Phase)

5.1.Compression between Traditional Technique and SBNN Model

Compression Point	Traditional Similarity Measurement Technique	Similarity-based Neural Network Model
Structure	The structure of the traditional technique is very simple.	The structure of the SBNN model is highly complex compare to the traditional technique.
Process	The structure of the technique is very simple which makes the process of similarity measurement fast.	The structure of the model is complex, several phases are involved to find the similarity between objects which makes the process complicated.
Technique	It used the Euclidian distance measurement technique for similarity measurement.	The SBNN model used the Minkowski distance measurement technique for similarity measurement.
Formula	Euclidian distance between two variables X and Y is defined as Distance (x,y)=($\sum Xi - Yi ^2$) ^{1/2}	Minkowski distance between two variables X and Y is defined as Distance (x,y)=($\sum Xi - Yi ^p$) ^{1/p} In this study, p=5 has been used to calculate distance.
Example	X = [4, 6] Y = [2, 5] Distance=2.2360679774998 Here, X and Y variables and the Euclidian distance between variables is 2.2360679774998. It is observed that the Euclidian distance formula is constant so the result of it also constant hence it is less capable to compute the efficient result for similarity measurement in the FBIR system.	X = [4, 6] Y = [2, 5] P=5 Distance=2.0800838230519 Here, X and Y variables and the Minkowski distance between variables is 2.0800838230519. It is observed that the Minkowski distance tries to find deeply nearest value as per requirement between them so it is more reliable to find the similarity between images in the FBIR system.
Performance	The traditional technique calculates the similarity between two objects in a single step so the performance of similarity measurement is good.	The SBNN model calculates the similarity between two objects using several phases so the process of similarity measurement takes time hence the performance of the SBNN model is low compare to the traditional technique.
Accuracy	The traditional technique calculates the similarity in a single step so the	In the SBNN model, the result of similarity measurement of two images depends on each

	accuracy level may be affected in some cases in a different situation.	band similarity result of images so the accuracy is more reliable than the traditional technique.
--	--	---

6. Conclusion

For effective image retrieval, recent image retrieval systems have been focused on multiple image features. Obtaining images from a multitude of semantic categories and datasets was an unavoidable necessity. To cater to the diverse image datasets, it is critical to retrieve images based on their rudimentary features such as shape, texture, colour, and spatial detail. Modern detectors and descriptors are capable of locating interest points depending on their field of expertise. In order to retrieve the noiseless and smooth image for post-processing, in this study, a similarity-based neural network model for feature-based image retrieval (FBIR) system has been developed. In the FBIR system, the user gives a query string as an input, and the feature database receives the query string and returns a set of feature values according to a query string. The FBIR system contains a repository of referenced images, which is used to map the similar features between a query image and a referenced image. The similarity measurement technique is used to measure the similarity between reference image features and a set of feature values that were returned by the feature database. Similarly, all feature values of the set interact with referenced image features. The FBIR system aligns the images in the grid based on the query string, and the similarity measurement result helps to identify the best possible images in the grid. The system allows the retrieval of the best possible images from the grid that can produce an efficient result. The user selects an image from the grid, and the system serves it (image retrieval) as a result. The crucial part of the system is similarity measurement, the developed model is capable to find similar bands between images, and based on similarity result the SBNN based FBIR system allows to retrieve best possible images from the repository that can produce an efficient and accurate result for earth surface monitoring. The main advantage of the new system that there will not be a need to download a complete image, the user can simply select the required individual band image and can easily download it through a developed user-friendly GUI. A distance measurement is the underlying property of a similarity-based neural network model, and the model relies on self-organizing maps. However, a distance measure implies some requirements on the data which are not always easy to satisfy in practice. In future, a similarity-based neural network (SBNN) model can be used for big data repository to find out the best suitable images for land surface monitoring.

7. Acknowledgement

The authors are thankful to the Advanced Computing & Research Laboratory, Department of Computer Application, Integral University, Lucknow, India for providing the necessary support to carry out the work. The manuscript communication number (MCN) is IU/R&D/2021-MCN0001134.

References

1. Alsmadi, M.K., Alsmadi. (2017). An efficient similarity measure for content based image retrieval using memetic algorithm. *Egyptian Journal of Basic and Applied Sciences*, 4(2), 112-122.
2. Ahmed, K.T., Ummesafi, S., Iqbal, A. (2019). Content based image retrieval using image features information fusion. *Information Fusion*, 51, 76-99.
3. Ahmed, T., Naidu, S.V., Singh, D., Raman, B. (2015). An Approach to Detect Hotspots with INSAT-3D Data," in *Proceeding of National Conference on Recent Advances in Electronics & Communication Engineering (RAECE 2015)*, at IIT Roorkee, India, pp. 267-270.
4. Arivazhagan, S., Anbazhagan, S. (2017). ASTER Data Analyses for Lithological Discrimination of Sittampundi Anorthositic Complex, Southern India. *Geosciences Research*, 2(3), 196-209.
5. Bunte, K., Biehl, M., Jonkman, M.F., Petkov, N. (2011). Learning effective color features for content based image retrieval in dermatology. *Pattern Recognition*, 44(9), 1892-1902.
6. Chan, Y.K., Chen, C.Y. (2004). Image retrieval system based on color-complexity and color-spatial features. *Journal of Systems and Software*, 71(1-2), 65-70.
7. Demirkesena, A.C., Hazelton, N.W.J., Sauder, D.M. (2004). AUTOMATING INTERPRETATION OF GEOLOGICAL STRUCTURES FROM LANDSAT TM MULTI-SPECTRAL IMAGES AND DEMs. *ISPRS*.
8. El-Naqa, I., Yang, Y., Galatsanos, N.P., Nishikawa, R.M., Wernick, M.N. (2004). A similarity learning approach to content-based image retrieval: application to digital mammography. *IEEE Transactions on Medical Imaging*, 23(10), 1233-1244.
9. ElAlami, M.E. (2014). A new matching strategy for content based image retrieval system. *Applied Soft Computing*, 14(C), 407-418.
10. Garcia, N., Vogiatzis, G. (2019). Learning non-metric visual similarity for image retrieval. *IEEE Transactions on Medical Imaging*, 38, 18-25.
11. Herráez, M.A., Domingo, J., Ferri, F.J. (2008). Combining similarity measures in content-based image retrieval. *Pattern Recognition Letters*, 29(16), 2174-2181.

12. Huang, Z.C., Chan, P.P.K., Ng, W.W.Y., Yeung, D.S. (2010). Content-Based Image Retrieval Using Color Moment And Gabor Texture Feature. Proc. IEEE Symp. International Conference on Machine Learning and Cybernetics, Qingdao, IEEE Press (pp. 719-724).
13. Inbaraj, R., Ravi, D.G. (2020). A Survey On Recent Trends In Content Based Image Retrieval System. Journal of Critical Reviews, 7(11), 961-965.
14. Kaur, M., Dhingra, S. (2017). Comparative analysis of image classification techniques using statistical features in CBIR systems. Proc. IEEE Symp. International Conference on I-SMAC (IoT in Social, Mobile, Analytics and Cloud) (I-SMAC), IEEE Press (pp. 265-270).
15. Lu, T.C., Chang, C.C. (2007). Color image retrieval technique based on color features and image bitmap. Information Processing & Management, 43(2), 461-472.
16. Ma, L., Liu, Y., Zhang, X., Ye, Y., Yin, G., Johnson, B.A. (2019). Deep learning in remote sensing applications: A meta-analysis and review. ISPRS Journal of Photogrammetry and Remote Sensing, 152, 166-177.
17. Malik, F., Baharudin, B. (2013). Analysis of distance metrics in content-based image retrieval using statistical quantized histogram texture features in the DCT domain. Applied Soft Computing, 25(2), 207-218.
18. Maggini, M., Melacci, S., Sarti, L. (2012). Learning from pairwise constraints by Similarity Neural Networks. Neural Networks, 26, 141-158.
19. Montanaro, M., Lunsford, A., Tesfaye, Z., Wenny, B., Reuter, D. (2014). Radiometric Calibration Methodology of the Landsat 8 Thermal Infrared Sensor. Remote Sens., 6(9), 8803-8821.
20. MO, D., ER, V. (2019). Performance Analysis of Distance Metric for Content Based Image Retrieval. International Journal of Engineering and Advanced Technology, 8(6), 2215-2218.
21. Palwe, S.A., Mishra, D. (2018). Color Image Retrieval Using Compacted Feature Vector with Mean-Count Tree. Procedia Computer Science, 132, 1739-1746.
22. Rasul, A., Balzter, H., Ibrahim, G.R.F., Hameed, H.M., Wheeler, J., Adamu, B., Ibrahim, S., Najmaddin, P.M. (2018). Applying Built-Up and Bare-Soil Indices from Landsat 8 to Cities in Dry Climates. Land, 7(3), 1-13
23. Sharma, P., Mutreja, U. (2013). Analysis of Satellite Images using Artificial Neural Network. International Journal of Soft Computing and Engineering, 173(3), 235-240.
24. Sutojo, T., Tirajani, P.S. Setiadi, D.R.I.M., Sari, C.A., Rachmawanto, E.H., (2017). CBIR for classification of cow types using GLCM and color features extraction. Proc. IEEE Symp. 2nd International conferences on Information Technology, Information Systems and Electrical Engineering (pp. 182-187).
25. Srivastava, S., Ahmed, T. (2021). Feature-Based Image Retrieval (FBIR) System for Satellite Image Quality Assessment Using Big Data Analytical Technique. Psychology and Education, 58(2), 10202-10220.
26. Thome, K.J. (2001). Absolute radiometric calibration of Landsat 7 ETM+ using the reflectance-based method. Remote Sensing of Environment, 78(1-2), 27-38.
27. Wang, X., Lee, F., Chen, Q. (2019). Similarity-preserving hashing based on deep neural networks for large-scale image retrieval. Journal of Visual Communication and Image Representation, 61, 260-271.
28. Wong, W.T., Hsu, S.H. (2006). Application of SVM and ANN for image retrieval. International Journal of Soft Computing and Engineering European Journal of Operational Research, 2(6), 938-950.
29. Wu, Z., Jiang, S., Zhou, X., Wang, Y., Zuo, Y., Wu, Z., Liang, L., Liu, Q., (2020). Application of image retrieval based on convolutional neural networks and Hu invariant moment algorithm in computer telecommunications. Computer Communications, 150, 729-738.
30. Xu, S., Li, C., Jiang, S. (2012). Similarity measures for content-based image retrieval based on intuitionistic fuzzy set theory. Journal of Computers, 7(7), 1733-1742.
31. Yuan, X., Liu, Q., Tesfaye, Z., Long, J., Hu, L., Wang, Y. (2019). Deep Image Similarity Measurement Based on the Improved Triplet Network with Spatial Pyramid Pooling. Information, 10(4), 1-17.
32. Yasmin, M., Mohsin, S., Sharif, M. (2014). Intelligent Image Retrieval Techniques: A Survey. Journal of Applied Research and Technology, 12(1), 87-103.
33. Yue, J., Li, Z., Liu, L., Fu, Z. (2011). Content-based image retrieval using color and texture fused features. Mathematical and Computer Modelling, 54(3-4), 1121-1127.